

## Vortex Configurations, Matching, and Domain Structure in Large Arrays of Artificial Pinning Centers

S. B. Field,<sup>1</sup> S. S. James,<sup>1,\*</sup> J. Barentine,<sup>1</sup> V. Metlushko,<sup>2,†</sup> G. Crabtree,<sup>2</sup> H. Shtrikman,<sup>3</sup> B. Ilic,<sup>4</sup> and S. R. J. Brueck<sup>4</sup>

<sup>1</sup>*Department of Physics, Colorado State University, Fort Collins, Colorado 80523*

<sup>2</sup>*MSD, Argonne National Laboratory, Argonne, Illinois 60439-4845*

<sup>3</sup>*Weizmann Institute of Science, Rehovot, Israel*

<sup>4</sup>*Center for High Technology Materials, University of New Mexico, Albuquerque, New Mexico 87131*

(Received 7 February 2000; published 28 January 2002)

High-resolution scanning Hall probe microscopy has been used to image vortex configurations in very large periodic arrays of artificial pinning sites. Strong matching effects are seen at fields where either one or two vortices can sit at a site; with three vortices per site, however, no clear matching is observed. Matching effects have also been observed at several fractional multiples of the matching field, including  $1/5$ ,  $1/4$ ,  $1/3$ ,  $1/2$ , and  $3/4$ . These fractional values are characterized by striking domain structure and grain boundaries.

DOI: 10.1103/PhysRevLett.88.067003

PACS numbers: 74.60.Ge, 74.25.Ha, 74.76.Db

The behavior of superconducting vortices in the presence of a periodic array of holes reveals rich and unexpected static and dynamic phenomena. In such arrays, flux can be quantized either “in” the holes (as a circulating current around their peripheries), or in the interstitial regions between the holes as ordinary Abrikosov vortices. At low fields, the holes act as very strong pinning centers for flux, and it is thus possible for holes to contain *multiquantum* vortices. However, the energy of such multiquantum vortices increases rapidly with the number of quanta  $n$  [1]. This leads to a *saturation number*  $n_s$ , beyond which it is energetically favorable for any additional flux to enter the interstitial regions between the holes as Abrikosov vortices. Transport [2–4] and magnetization [5–9] studies show distinctive features at matching fields where the vortex structure is commensurate with the hole array. Interesting configurations also arise at fractional matching fields, where the occupation number of each hole or the number of interstitial vortices forms a superstructure locked to the basic hole array [5,9].

Although magnetization and transport studies have elucidated much of the basic phenomenology of the array/vortex system, they can measure only its *global* properties and cannot deduce details of the *local configurational* vortex state. Recently, Lorentz [10] and scanning Hall probe [11] microscopies have been used to image vortex configurations, but only over relatively small areas of  $\approx 10 \times 10$  pinning sites. In this Letter, we present large-area scanning Hall probe microscope (SHM) images of vortex configurations in arrays containing  $\approx 10^6$  holes. Our images span some 5000 holes, and so yield important information on the *large-scale* structure of the vortex configurations. These studies reveal striking multiquantum and interstitial vortex patterns in a square-periodic hole array. At fractional matching fields, we resolve distinctive domains of phase-slip related vortex superstructures that are separated by domain walls with characteristic internal structure.

The Hall probe’s active area coupled with its scan height above the surface yield an effective FWHM resolution of  $3.4 \mu\text{m}$ . The sample investigated was a 100-nm-thick niobium film with  $0.3\text{-}\mu\text{m}$ -diameter holes on a square lattice. The lattice constant  $a$  was  $1.870 \mu\text{m}$ , yielding an expected first matching field  $H_m = \Phi_0/a^2 = 5.913 \text{ G}$ . The array was produced using a lithographic technique based on the interference of light [8], which yields very large and uniform arrays (here  $\approx 2 \text{ mm} \times 3 \text{ mm}$ ). Our data were taken far from the edges of the array. Takezawa and Fukushima [12] have calculated the pinning energy of a hole vortex relative to one in the bulk. For parameters similar to ours, they find a very deep pinning potential of  $\approx 100 \text{ eV}$ . Comparing this to typical bulk Nb pinning energies of  $\approx 50 \text{ meV}$  [13], it is clear that pinning from the hole array dominates pinning from defects in the Nb film.

SHM images near several matching fields are shown in Fig. 1. For each image, the samples were field cooled from above  $T_c = 8.37 \text{ K}$  to a base temperature below  $3 \text{ K}$  where the images were taken. The top row of Fig. 1 shows the progression in the vortex configurations as the applied field  $H$  is varied around  $\bar{H} \equiv H/H_m = 0$ . At  $\bar{H} \approx 0$  we see several isolated vortices (dark spots). The actual vortex diameter is much smaller than these spots, whose size is determined by the Hall probe resolution. A somewhat darker spot, just to the right and below center, appears in all scans and is presumably associated with a physical defect in the hole lattice, which allows extra flux to sit at that point. As the field is increased from zero, vortices begin to enter the sample in larger numbers, as seen in the  $\bar{H} = 0.075$  and  $0.15$  images. A similar progression is observed for *negative* field increments away from zero, as shown at  $\bar{H} = -0.075$  and  $-0.15$ . Here the vortices appear as light spots, indicating that they are oppositely directed to those seen in positive fields.

As we continue to increase the field towards what we will be able to identify as the first matching field  $H_m$

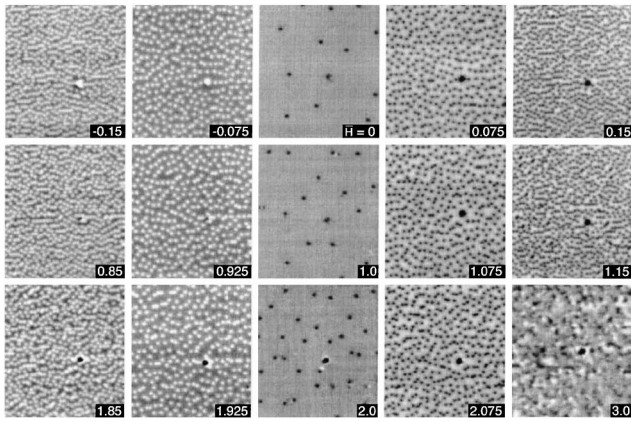


FIG. 1. SHM images obtained at applied magnetic fields  $H$  near the matching fields  $\bar{H} \equiv H/H_m = 1, 2,$  and  $3$ . The scans are  $124 \mu\text{m} \times 138 \mu\text{m}$ , contain some 5000 holes, and have a full scale of  $0.73 \text{ G}$ . Note the striking similarity between the vortex configurations near  $\bar{H} = 1$  and  $2$  and those near  $\bar{H} = 0$ . The smooth backgrounds at  $\bar{H} = 1$  ( $2$ ) consist of holes uniformly filled with  $1$  ( $2$ ) vortices. At  $\bar{H} = 3$ , however, the vortex configuration is highly disordered because of weakly pinned interstitials competing with vortices in holes. The dark black spot is a local defect in the sample.

( $\bar{H} = 1$ ), we begin to see a very remarkable progression (Fig. 1, second row). For instance, at an applied field of  $\bar{H} = 0.85 = 1 - 0.15$ , the image looks statistically identical to the image at  $\bar{H} = -0.15$ . And, remarkably, the image at  $\bar{H} = 1$  is essentially indistinguishable from that at  $\bar{H} = 0$ . It is important to note here that in each image the average value of the field has been subtracted out. This is why the  $\bar{H} = 1$  image at about  $6 \text{ G}$  and the  $\bar{H} = 0$  image appear to have about the same overall gray level. We can then understand the appearance of the  $\bar{H} = 1$  scan as follows. The field increment from an exactly  $H = 0$  image (no spots) to the next no-spot image is  $5.929 \text{ G}$ , very close to the first matching field of  $5.913 \text{ G}$  deduced from the lattice geometry. Thus, we identify this later spot-free image at  $5.929 \text{ G}$  with the first matching field or  $\bar{H} \equiv 1$ . The smooth gray background near  $\bar{H} = 1$  can then be explained in the following way. Exactly at  $\bar{H} = 1$ , each hole contains exactly one vortex, leading to a dense and uniform configuration of vortices. The spatial resolution of our Hall probe is not good enough to image individual vortices when they are this close together *and perfectly ordered* [14], so this regular array of vortices appears as a smooth gray background. The few black spots in the  $\bar{H} \approx 1$  image are thus (easily visible) *extra* vortices.

The third row of Fig. 1 shows the vortex configurations as the field is further increased through the second matching field ( $\bar{H} = 2$ ). A very similar progression is observed. At  $\bar{H} \approx 2$ , there is again a smooth background populated by a few black spots. Again, we interpret this background as the highly ordered state with now *two* vortices sitting in each hole; black spots for  $\bar{H} > 2$  are again extra vortices, and white spots for  $\bar{H} < 2$  now represent a hole with only

*one* vortex. At the *third* matching field ( $\bar{H} = 3$ ), however, the appearance is radically different (Fig. 1, bottom right). Instead of the smooth gray background we would expect if three vortices sat in each hole, we see a rather muddled image with no discernible structure. We believe this different appearance results from the sudden presence of *interstitial* vortices above  $\bar{H} = 2$ .

To probe this issue more directly, we have taken close-up scans just below and above  $\bar{H} = 2$ . Figure 2(a) shows a  $25 \mu\text{m} \times 28 \mu\text{m}$  scan at a field  $\bar{H} = 2 - 0.084$ , and Fig. 2(b) shows  $\bar{H} = 2 + 0.084$ . Also shown is the least-squares-fit positions of the holes as determined from an image taken at  $\bar{H} = 1/2$  where the hole positions are unambiguous [see, e.g., Fig. 3(b)]. We also have used an absolute position sensor [15] mounted on the scanner head to compensate for any possible drifts between images. In Fig. 2(a) each white spot (i.e., a “missing” vortex) clearly sits directly on a hole, indicating as well that all *vortices* also sit on the holes. However, in Fig. 2(b) the black spots, which are now extra vortices, sit variously on holes *or* on interstitial sites.

Large holes “spread out” the fields of the hole vortices, lowering their energies and leading to stronger pinning. Thus the maximum number of vortices  $n_s$  that can occupy a hole depends on the hole radius  $R$  [1,16]. With the sputtering/lift-off lithography used here [8], there will be inevitable fluctuations in the hole diameters, perhaps yielding  $n_s = 2$  for some holes and  $n_s = 3$  for others. Vortices nucleating near  $n_s = 2$  holes would end up as interstitials, while those near  $n_s = 3$  sites could sit in a hole. This random-appearing admixture of vortices on holes and in interstitial sites would, by  $\bar{H} = 3$ , lead to the very disordered configuration observed at that field (Fig. 1).

It is also possible to have matching effects at noninteger multiples of  $H_m$ . Indeed, distinct features at  $\bar{H} = 1/4, 1/2,$  and possibly  $1/5$  (or  $3/16$ ),  $1/8,$  and  $1/16$  have

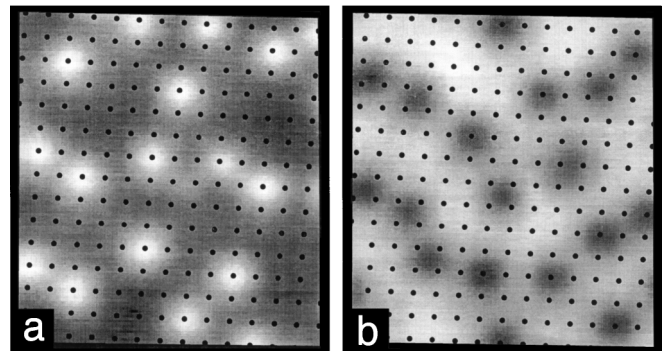


FIG. 2. Vortex configurations (a) just below ( $\bar{H} = 1.916$ ) and (b) just above ( $\bar{H} = 2.084$ ) the second matching field. The small dark circles are the positions of the holes. Below  $\bar{H} = 2$ , the vacancies (white spots) all sit directly on holes; thus all vortices must as well. Above  $\bar{H} = 2$ , the extra vortices (dark spots) sit on both hole *and* interstitial sites.  $25 \mu\text{m} \times 27 \mu\text{m}$  field is shown.

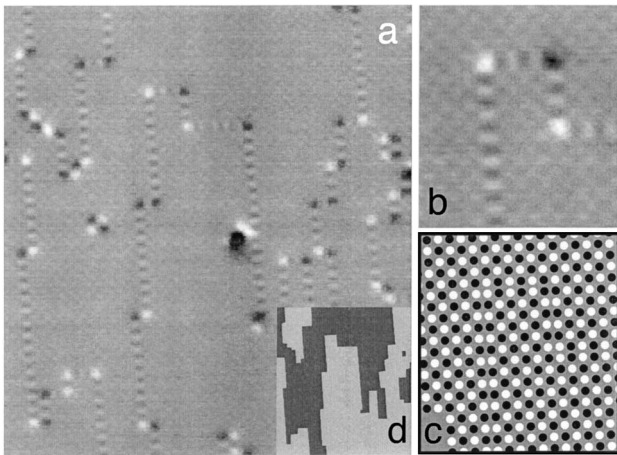


FIG. 3. (a)  $122 \mu\text{m} \times 138 \mu\text{m}$  image of the vortex configuration at  $\bar{H} = 1/2$ . There are large areas of vortices arranged in a checkerboard pattern; domains [outlined in (d)] of opposite checkerboard polarity are separated by stripelike grain boundaries. A close-up of this configuration is shown in (b) and schematically in (c).

been observed in magnetization studies [5,17], and Harada *et al.* [10] have imaged noninteger matching at  $1/4$ ,  $1/2$ ,  $3/2$ , and  $5/2$ . In our imaging experiments, we also observe matching effects at several of these fractional fields, as well as some not previously observed. We find that vortex configurations at fractional matching fields are characterized by striking domain structure and associated grain boundaries.

By far the strongest submatching effects occur at  $\bar{H} = 1/2$ . Figure 3(a) shows that the configuration consists of large areas of well-matched vortices separated by curious stripelike boundaries. The close-up in Fig. 3(b) reveals that the smooth regions consist of vortices occupying every other hole in a checkerboardlike fashion. Regions of different “polarity”—with the vortices occupying either the “red” or “black” squares of the checkerboard—are separated by striped grain boundaries [18]. Figure 3(c) schematically shows how a polarity shift results in rows or columns of alternating *pairs* of vortices and vacancies, which appear in the images as the striking boundary features. At the junctions between north-south and east-west boundaries, there is always a bright or dark spot, whose origin is again clear from Fig. 3(c). From considerations of the boundaries, we have mapped out the domains of differing polarity [inset, Fig. 3(a)]. One curious feature of these grain boundaries is that they run predominately north-south, indicating a breaking of the square symmetry of the lattice in these two directions. Our images demonstrate that the simple domain wall structure seen on small scales [11] yields unexpectedly complex patterns on large scales.

Weaker but still striking matching effects occur at  $\bar{H} = 1/4$  as well as its *complimentary* [19] field of  $\bar{H} = 1 - 1/4 = 3/4$  (Fig. 4). Zooming in on the boundary of such a patch [outlined in Figs. 4(a) and 4(b)] allows us to explore

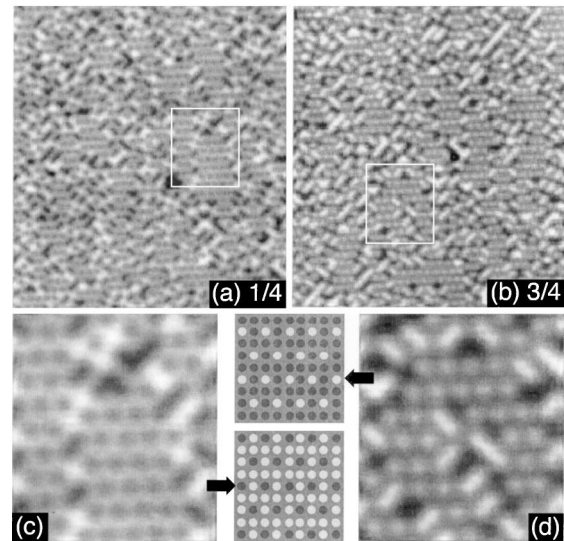


FIG. 4.  $122 \mu\text{m} \times 136 \mu\text{m}$  images of vortex configurations at  $\bar{H} = 1/4$  (a) and  $3/4$  (b). Selected regions are expanded in (c) and (d). The configurations consist of relatively small well-ordered regions surrounded by complex disordered boundaries. Also shown schematically are the inferred vortex arrangements in the ordered regions. Light circles represent empty holes, and dark circles occupied holes.

the vortex configuration in detail [Figs. 4(c) and 4(d)]. The vortex configuration in the ordered regions is shown to scale schematically in Fig. 4. Notice that the configuration may be viewed in terms of alternating empty and half-filled rows [10,20]; this again indicates the presence of a symmetry-breaking field which selects this particular grain orientation. One possible source of this asymmetry could be a small difference in the interhole spacing  $a$  in the horizontal and vertical directions. However, no such asymmetry is visible at the  $\approx 0.1\%$  accuracy of our optical diffraction measurements of  $a$ .

The origin of the intricate vortex patterns at submatching fields can be understood from their configurational energies. In our samples, the vortex spacing is large compared to the penetration depth and the energy of a configuration can be estimated from nearest-neighbor interactions only. At  $1/2$  filling, the observed vertical and horizontal domain walls contain nearest neighbors on half the lattice sites, whereas a  $45^\circ$  boundary, for example, would have nearest neighbors on all the lattice sites along the boundary and thus represent a much higher energy. The energy of the domain wall is considerably higher than that of the ordered phases where neighboring lattice sites are never occupied. This favors few boundaries and large ordered regions, as observed. In contrast, at  $1/4$  filling the vortices are substantially farther apart, lowering their repulsive energy. The energy differences between domain walls and ordered phases are less pronounced, and the possible domain wall configurations are also closer in energy. Therefore more domain wall configurations appear with greater frequency than at  $1/2$ .

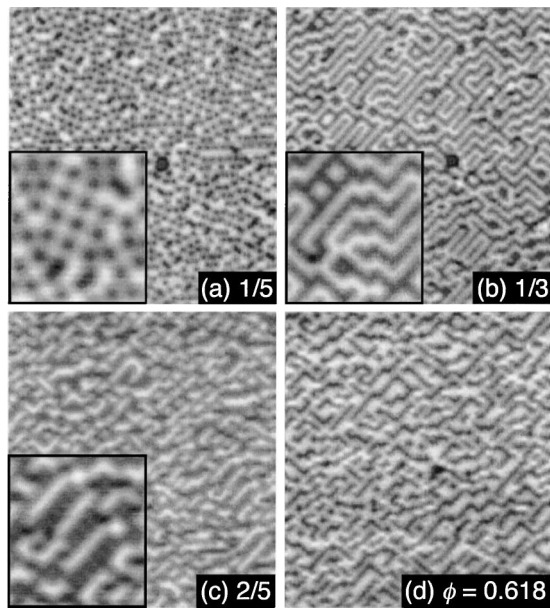


FIG. 5.  $122 \mu\text{m} \times 137 \mu\text{m}$  images of vortex configurations at several fractional values of  $\bar{H}$ . Also shown is the “irrational” field  $\phi = (\sqrt{5} - 1)/2$ .

Intuitive analysis is less obvious at other fractions (Fig. 5), but one can turn to simulations for guidance. At  $1/3$  filling, Reichhardt and Grønbech-Jensen [21] find a disordered state containing many filled  $45^\circ$  diagonal rows separated by two empty diagonals, as seen in Fig. 5(b). An ordered structure of this type has also been predicted by Watson [20] for a “zero range” repulsive potential and by Teitel and Jayaprakash [22] in superconducting wire networks. At  $1/5$  filling, filled diagonals at  $\arctan(1/2) = 26.6^\circ$  separated by four empty diagonals are the lowest energy configuration [5,20,21]. Again, since the vortex density is low, other configurations have only slightly higher energies and occur frequently. The same kinds of imperfect diagonal structures of filled and empty rows can be seen at  $2/5$  filling [Fig. 5(c)], and at the irrational field of  $(\sqrt{5} - 1)/2 \approx 0.618$  [Fig. 5(d)], indicating their relatively low configurational energies. The frequent occurrence of configurational disorder obscures any long-range distinction between rational and irrational filling in Fig. 5.

Vortex configurations in square-periodic hole arrays thus reveal remarkably complex patterns reflecting the interplay between the pinning energy of the hole array and the interaction energy of the multiquantum and interstitial flux structures. Our images show clear multiquantum occupation of the holes up to saturation, followed by the appearance of interstitial Abrikosov vortices at higher fields. At fractional filling factors, domains of well-ordered vortices are separated by a network of domain boundaries displaying remarkably simple order for half filling and

increasing complexity at other fillings. There appears to be a nontrivial set of ordered fractional states, a complete inventory of which awaits a general theory correctly incorporating the several competing interactions present. Similar to other collective vortex phenomena, these competing ground states can be mapped onto a variety of statistical models that describe the basic phenomena of many other condensed matter systems [23].

We would like to acknowledge helpful discussions with C. Reichhardt and C. Olson. This work was supported by NSF Grant No. DMR-9701532 (S.B.F., S.S.J., J.B.) and the U.S. Department of Energy, Office of Basic Energy Sciences-Materials Sciences, under Contract No. W-31-ENG-38 (V.M., G.W.C.).

\*Present address: IRC in Superconductivity, Madingley Road, Cambridge CB3 0HE, United Kingdom.

†Present address: Department of Electrical Engineering and Computer Science, University of Illinois at Chicago, Chicago, IL 60607-0024.

- [1] G. S. Mkrtychyan and V. V. Shmidt, *Sov. Phys. JETP* **34**, 195 (1972).
- [2] A. T. Fiory, A. F. Hebard, and S. Somekh, *Appl. Phys. Lett.* **32**, 73 (1978).
- [3] L. Van Look *et al.*, *Phys. Rev. B* **60**, R6998 (1999).
- [4] T. Puig *et al.*, *Phys. Rev. B* **58**, 5744 (1998).
- [5] M. Baert *et al.*, *Europhys. Lett.* **29**, 157 (1995).
- [6] V. V. Moshchalkov, *Phys. Rev. B* **54**, 7385 (1996).
- [7] V. V. Moshchalkov *et al.*, *Phys. Rev. B* **57**, 3615 (1998).
- [8] V. Metlushko *et al.*, *Phys. Rev. B* **59**, 603 (1999).
- [9] V. Metlushko *et al.*, *Phys. Rev. B* **60**, R12 585 (1999).
- [10] K. Harada *et al.*, *Science* **274**, 1167 (1996).
- [11] A. N. Grigorenko *et al.*, *Phys. Rev. B* **63**, 052504 (2001).
- [12] N. Takezawa and K. Fukushima, *Physica (Amsterdam)* **228C**, 149 (1994).
- [13] C.-H. Sow, K. Harada, A. Tonomura, G. Crabtree, and D. G. Grier, *Phys. Rev. Lett.* **80**, 2693 (1998).
- [14] D. Davidovic *et al.*, *Phys. Rev. B* **55**, 6518 (1996).
- [15] S. B. Field and J. Barentine, *Rev. Sci. Instrum.* **71**, 2603 (2000).
- [16] H. Nordborg and V. M. Vinokur, *Phys. Rev. B* **62**, 12 408 (2000).
- [17] V. Metlushko *et al.*, *Solid State Commun.* **91**, 331 (1994).
- [18] C. Reichhardt *et al.*, *Phys. Rev. B* **54**, 16 108 (1996).
- [19] Indeed, for *all* configurations observed at fractional field  $\bar{H} < 1$ , essentially identical configurations (with vortices and vacancies exchanged) are observed at a field  $1 - \bar{H}$ .
- [20] G. I. Watson, *Physica (Amsterdam)* **246A**, 253 (1997).
- [21] C. Reichhardt and N. Grønbech-Jensen, *Phys. Rev. B* **63**, 054510 (2001).
- [22] S. Teitel and C. Jayaprakash, *Phys. Rev. B* **27**, 598 (1983).
- [23] G. Blatter, M. V. Feigel'man, V. B. Geshkenbein, A. I. Larkin, and V. M. Vinokur, *Rev. Mod. Phys.* **66**, 1125 (1994).